

## **Co-doping NiP<sub>2</sub> as efficient and robust bifunctional electrocatalyst for overall water splitting in alkali and seawater**

Xiaoyu Hao,<sup>†a,b</sup> Qian Sun,<sup>†a</sup> Tianyi Zhang,<sup>a</sup> Panpan Song,<sup>c</sup> Jinglun Guo,<sup>a</sup> Svetlana Peshayad,<sup>d</sup> Longlong Chen,<sup>e</sup> Xiaolei Huang,<sup>\*c</sup> Xuqing Liu<sup>\*a,b</sup>

<sup>a</sup> State Key Laboratory of Solidification Processing, Centre of Advanced Lubrication and Seal Materials, Northwestern Polytechnical University, Xi'an 710072, China

<sup>b</sup> Shandong Laboratory of Advanced Materials and Green Manufacturing at Yantai, Yantai 264006, China

<sup>c</sup> Key Laboratory of Rare Earths, Ganjiang Innovation Academy, Chinese Academy of Sciences, Ganzhou 710043, China.

<sup>d</sup> al-Farabi Kazakh National University, Faculty of Physics and Technology, Almaty 050040, Kazakh.

<sup>e</sup> China National Petroleum Corporation Qinghai Oilfield Branch, Qinghai 817500, China

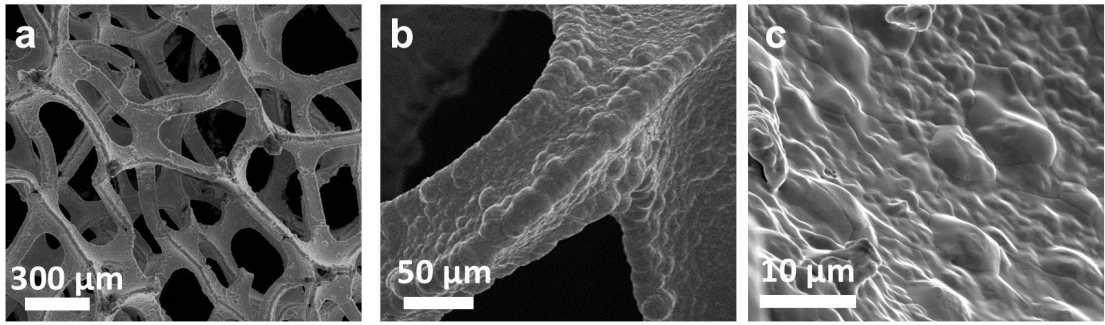


Fig.S1 SEM images of NF.

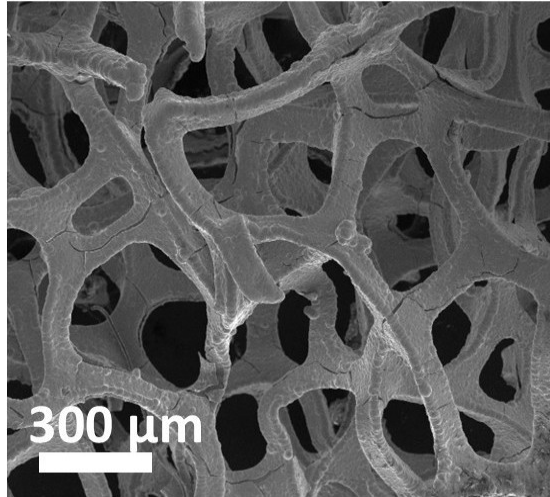


Fig.S2 SEM of Co<sub>8</sub>-NiP<sub>2</sub>.

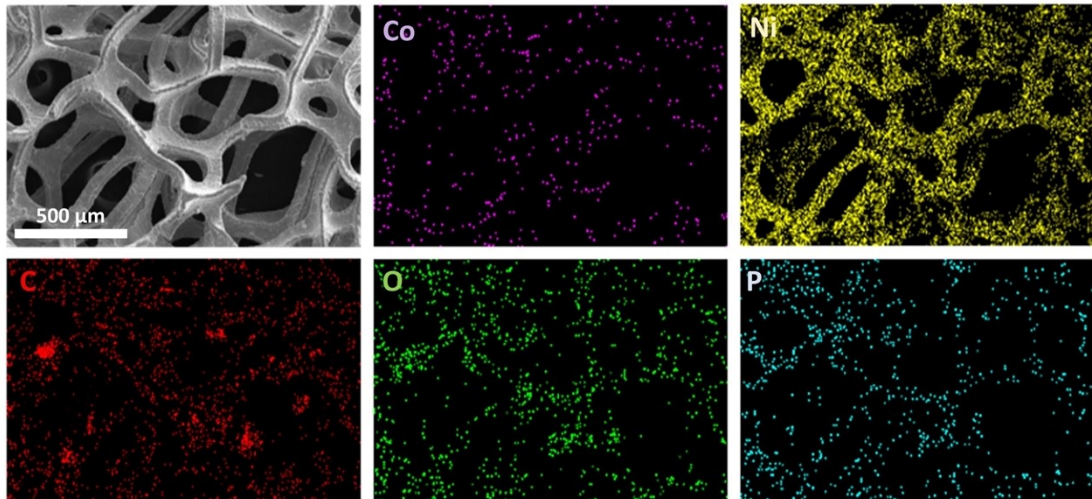


Fig.S3 EDS mapping of  $\text{Co}_8\text{-NiP}_2$ .

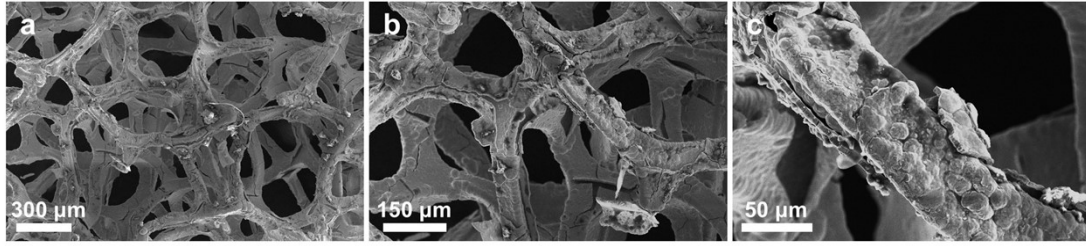


Fig.S4 SEM images of NiP<sub>2</sub>.

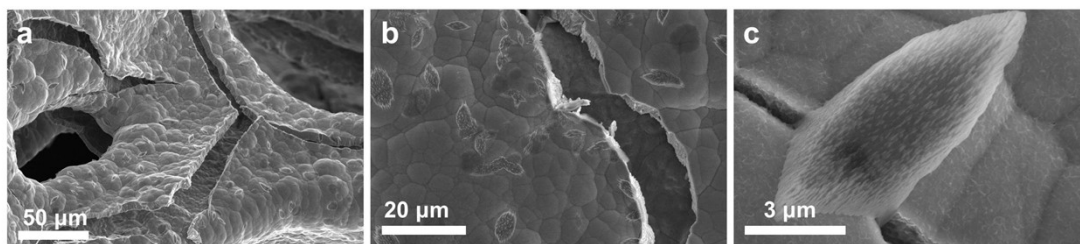


Fig.S5 SEM images of Co<sub>2</sub>-NiP<sub>2</sub>.

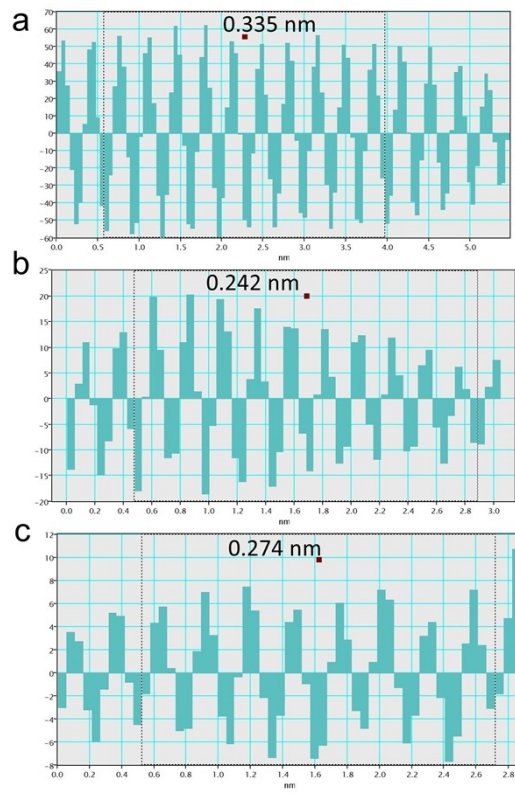


Fig.S6 Calculation of lattice spacing of  $\text{Co}_8\text{-NiP}_2$ .

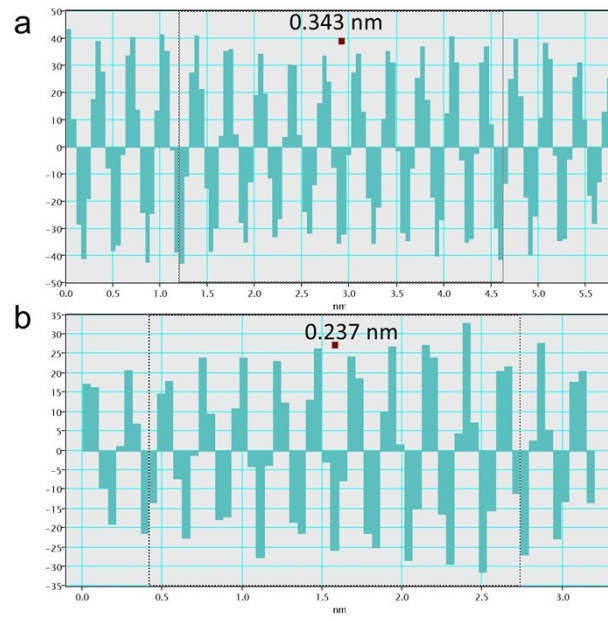


Fig.S7 Calculation of lattice spacing of NiP<sub>2</sub>.



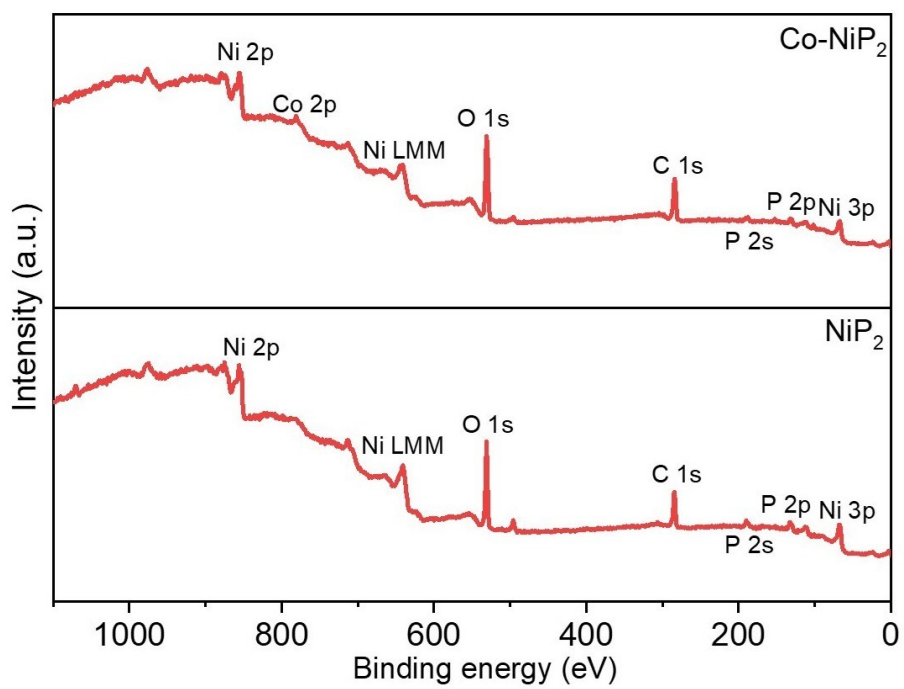


Fig.S9 XPS spectra of NiP<sub>2</sub> and Co<sub>8</sub>-NiP<sub>2</sub>

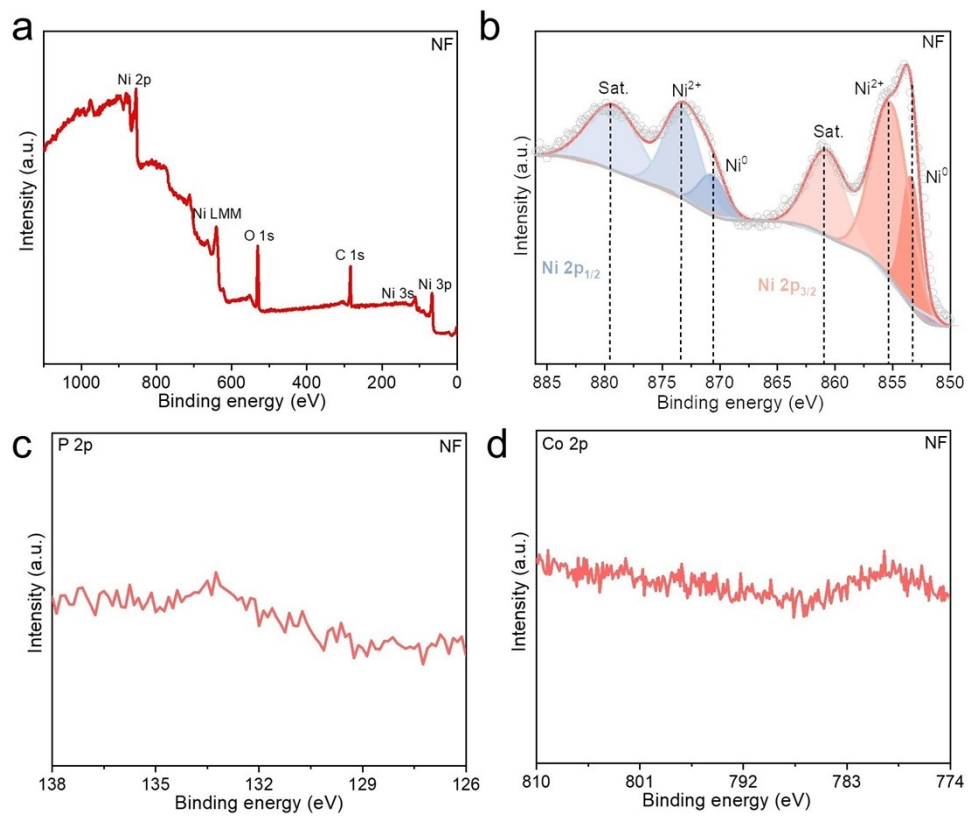


Fig.S10 (a) XPS spectra of NF. High resolution of (b) Ni 2p, (c) P 2p, (d) Co 2p.

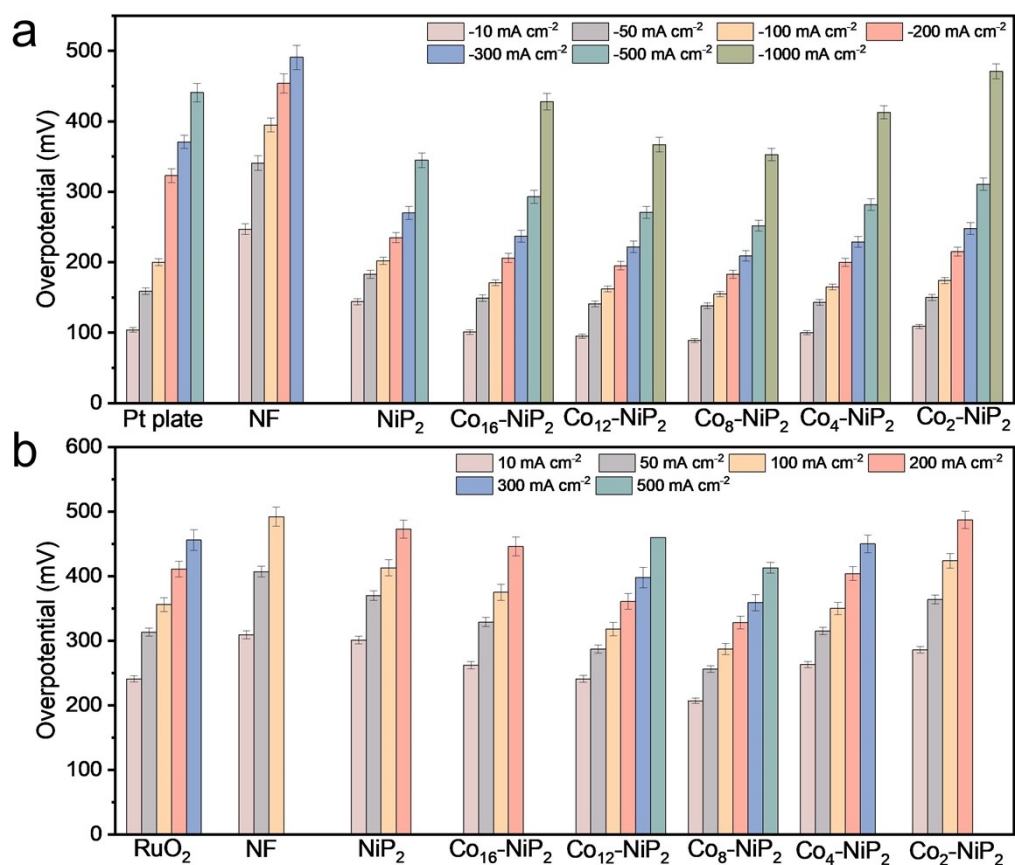


Fig.S11 Overpotential comparison of (a) HER and (b) OER in 1 M KOH.

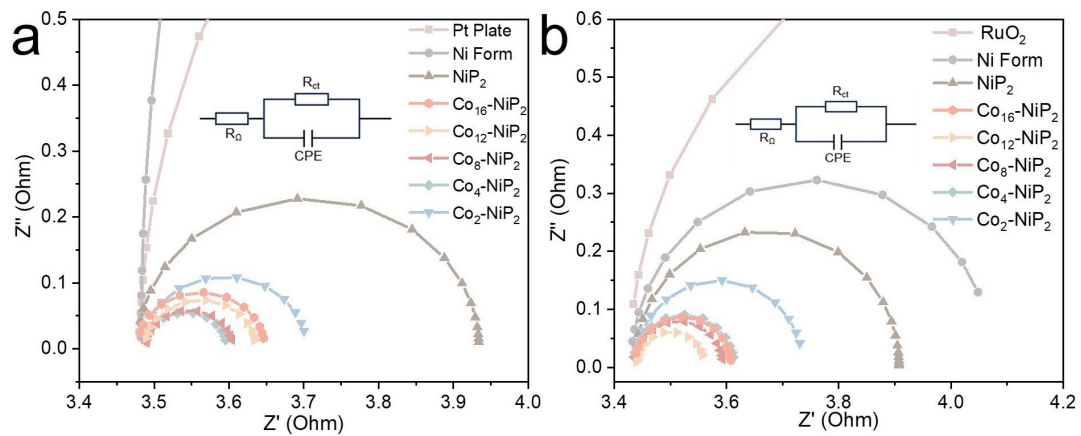


Fig.S12 Nyquist plot of (a)HER and (b) OER.

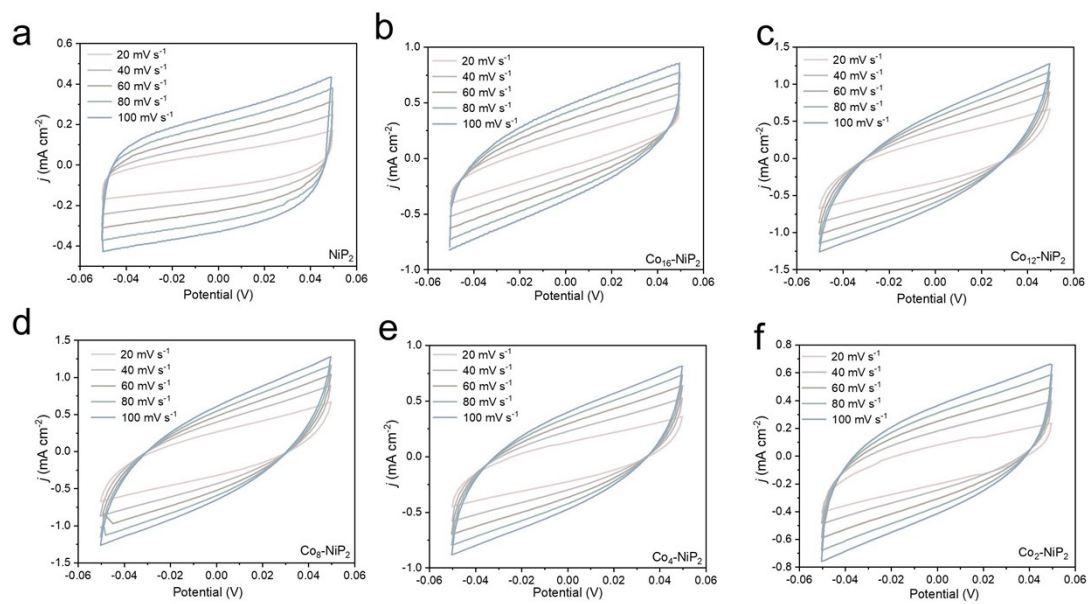


Fig.S13 CV curves at the scan rate of 20, 40, 60, 80, 100  $\text{mV s}^{-1}$  of HER process.

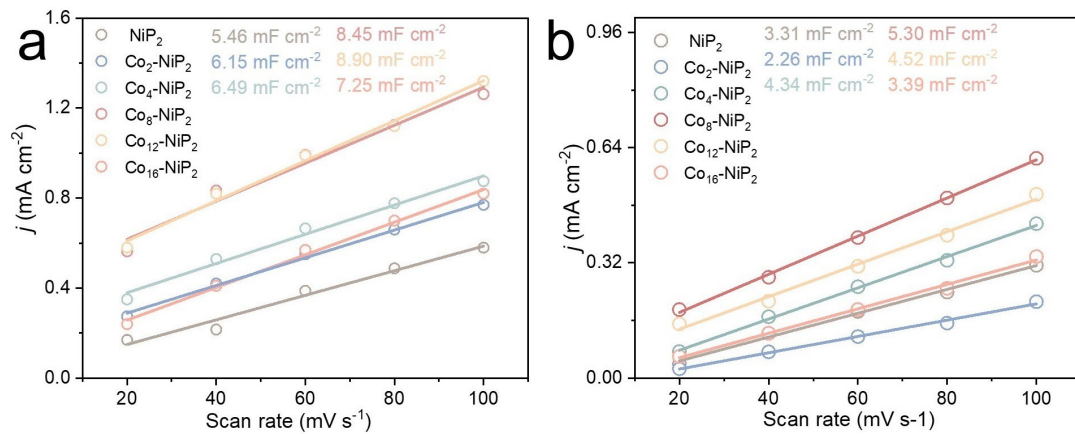


Fig.S14  $C_{dl}$  values of (a) HER catalysts and (b) OER catalysts.

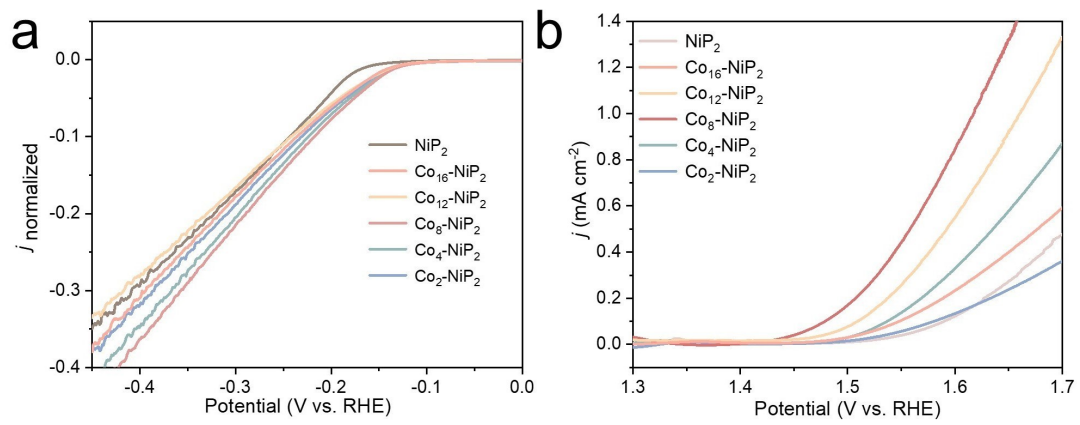


Fig.S15 The normalized polarization curves of ECSA of (a) HER and (b) OER.

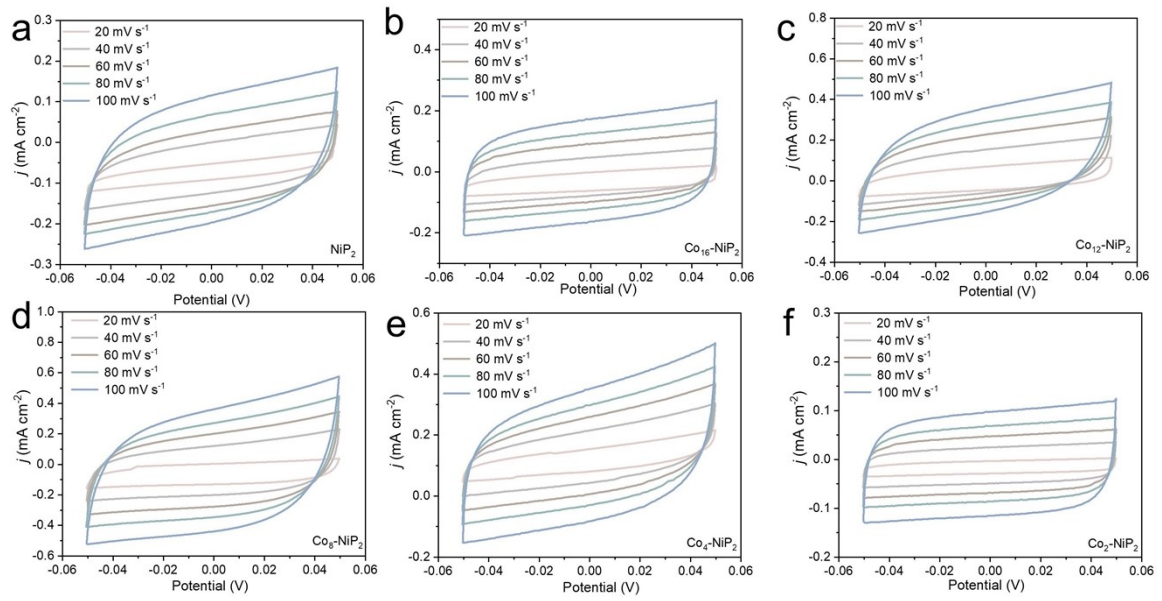


Fig.S16 CV curves at the scan rate of 20, 40, 60, 80, 100  $\text{mV s}^{-1}$  of OER process.

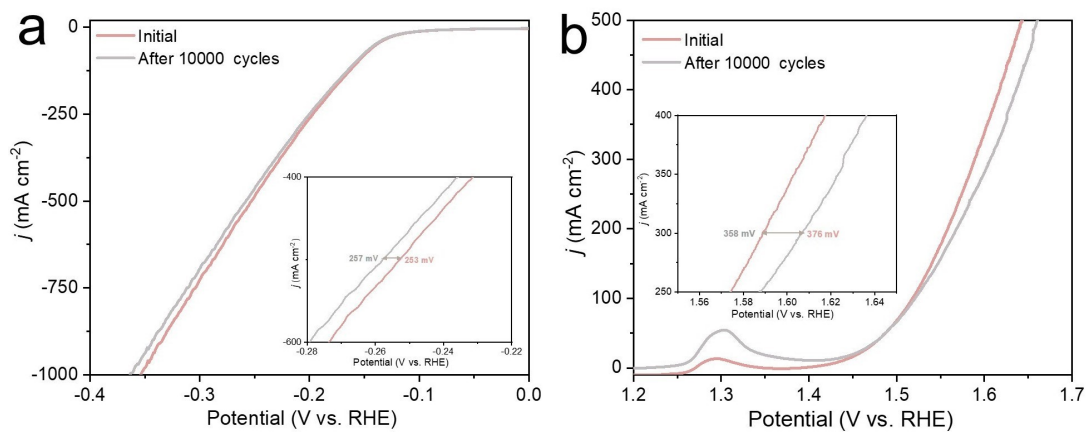


Fig.S17 Polarization curve of (a) HER and (b) OER before and after 10000 cycles.

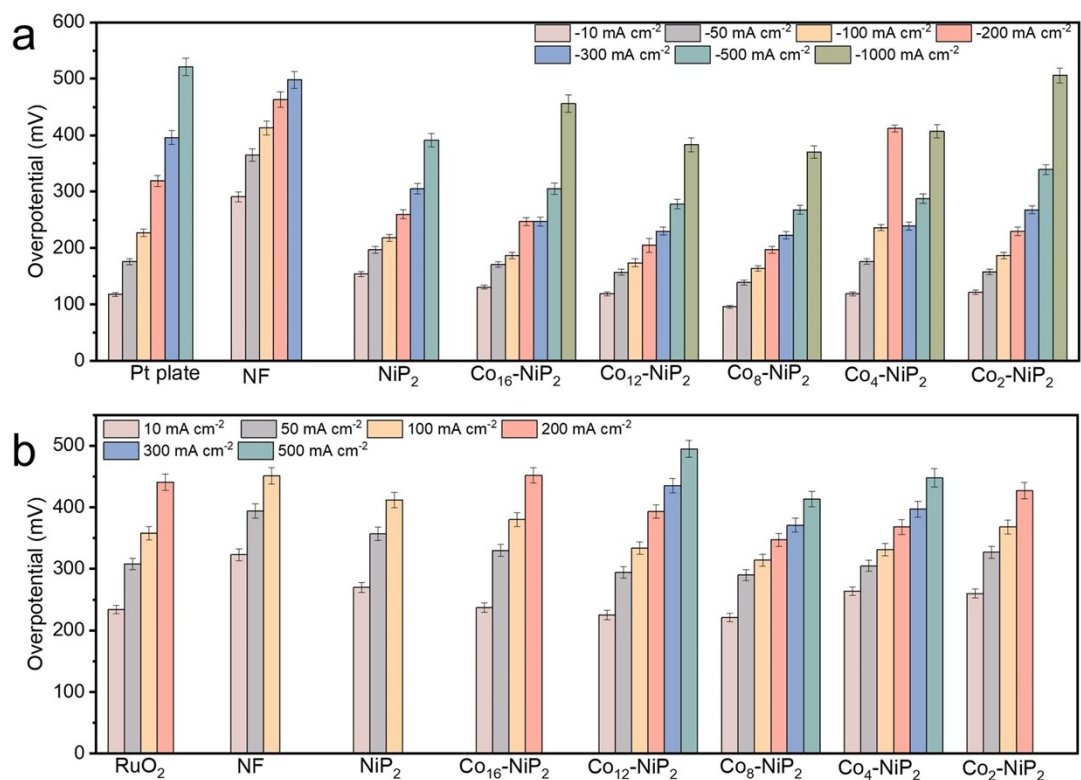


Fig.S18 Overpotential comparison of (a) HER and (b) OER in alkaline seawater.

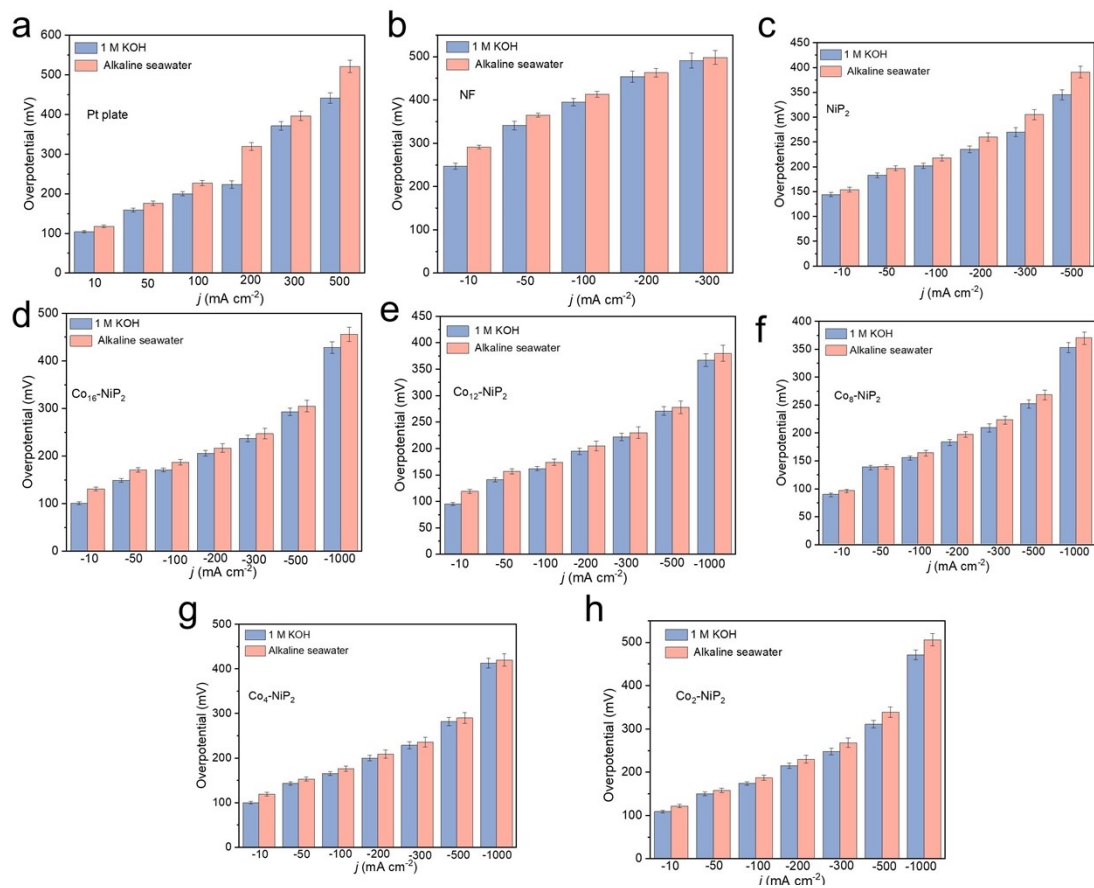


Fig.S19 Overpotential comparison of (a) Pt plate, (b) NF, (c) NiP<sub>2</sub>, (d) Co<sub>16</sub>-NiP<sub>2</sub>, (e) Co<sub>12</sub>-NiP<sub>2</sub>, (f) Co<sub>8</sub>-NiP<sub>2</sub>, (g) Co<sub>4</sub>-NiP<sub>2</sub>, (h)Co<sub>2</sub>-NiP<sub>2</sub> in 1 M KOH and alkaline seawater for HER.

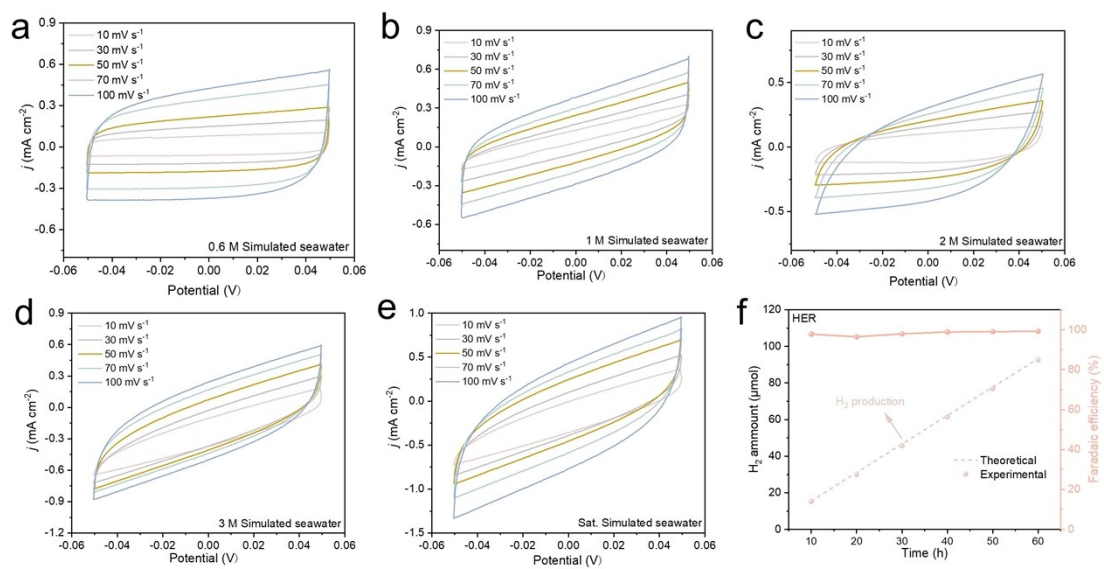


Fig.S20 CV curves at the scan rate of 20, 40, 60, 80, 100  $\text{mV s}^{-1}$  of  $\text{Co}_8\text{-NiP}_2$  for HER in (a) 0.6 M, (b) 1 M, (c) 2 M, (d) 3 M, (e) saturated simulated seawater. (f) Faraday efficiency.

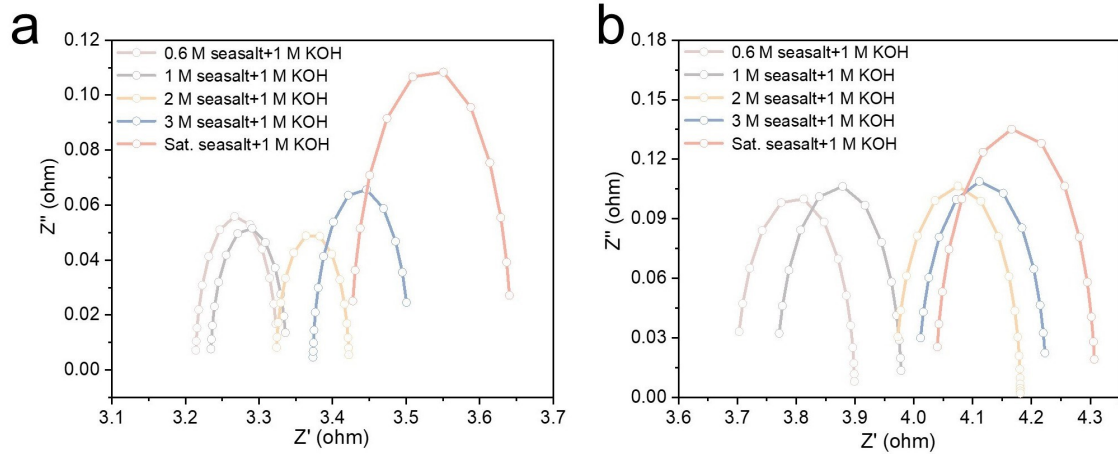


Fig.S21 Nyquist plot of (a)HER and (b) OER at simulated seawater of different concentrations.

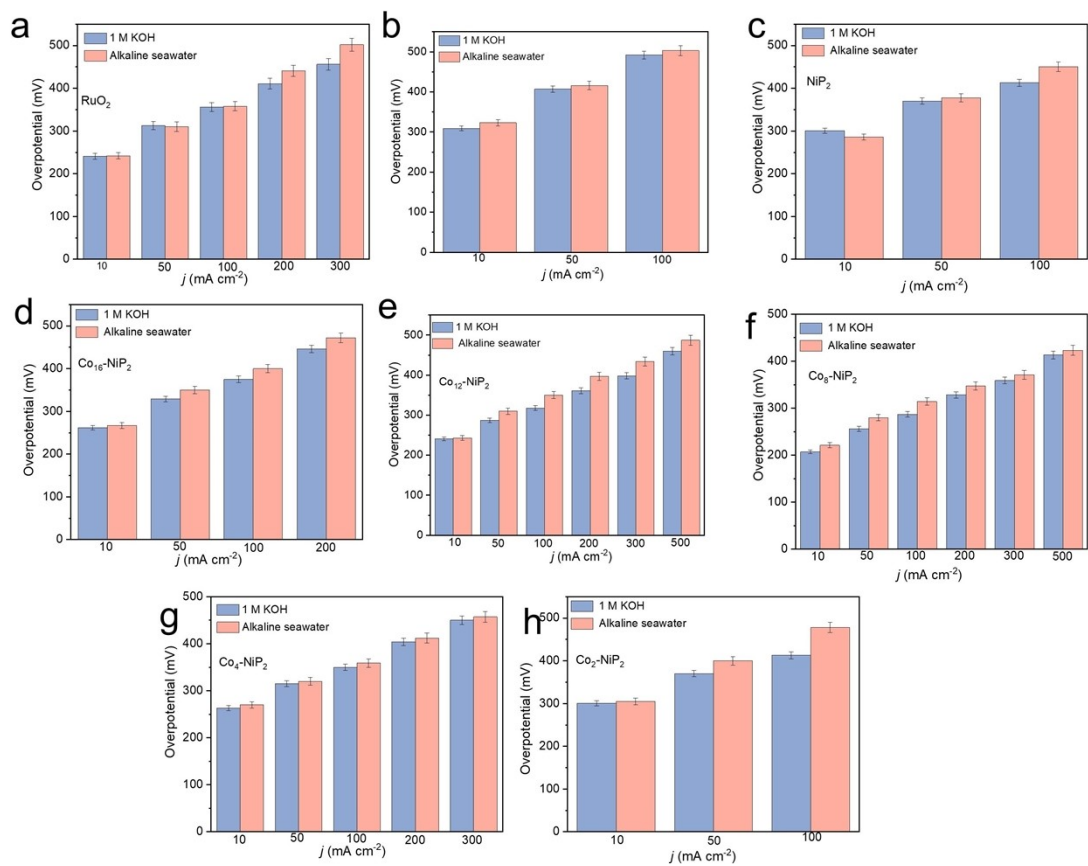


Fig.S22 Overpotential comparison of (a) RuO<sub>2</sub>, (b) NF, (c) NiP<sub>2</sub>, (d) Co<sub>16</sub>-NiP<sub>2</sub>, (e)

Co<sub>12</sub>-NiP<sub>2</sub>, (f) Co<sub>8</sub>-NiP<sub>2</sub>, (g) Co<sub>4</sub>-NiP<sub>2</sub>, (h) Co<sub>2</sub>-NiP<sub>2</sub> in 1 M KOH and alkaline

seawater for OER.

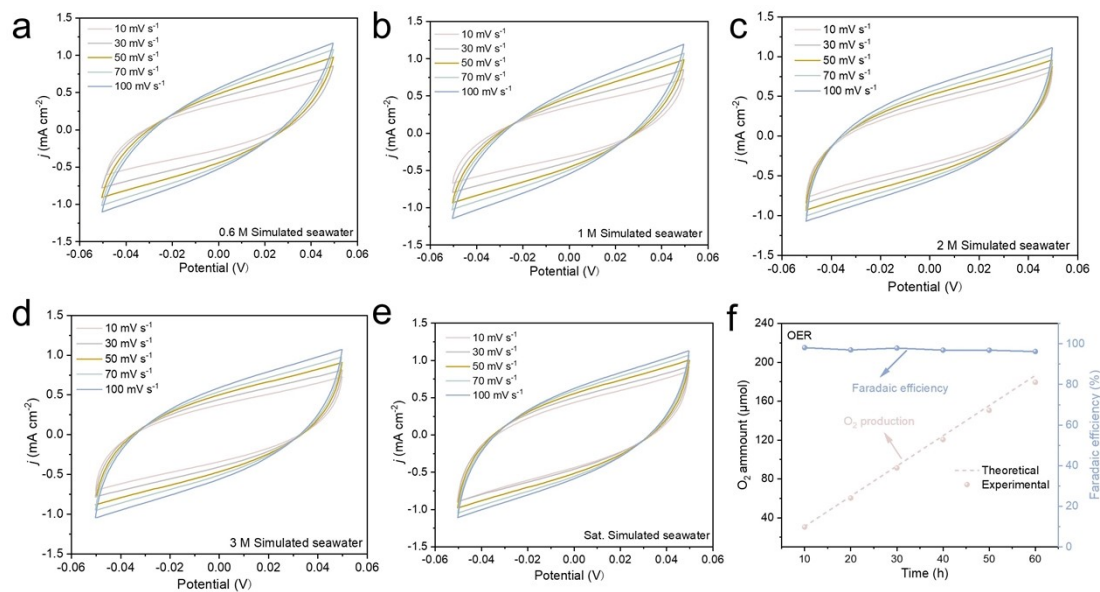


Fig.S23 CV curves at the scan rate of 20,40,60,80,100  $\text{mV s}^{-1}$  of  $\text{Co}_8\text{-NiP}_2$  for OER in (a) 0.6M, (b) 1M, (c) 2M, (d) 3M, (e) saturated simulated seawater. (f) Faraday efficiency.

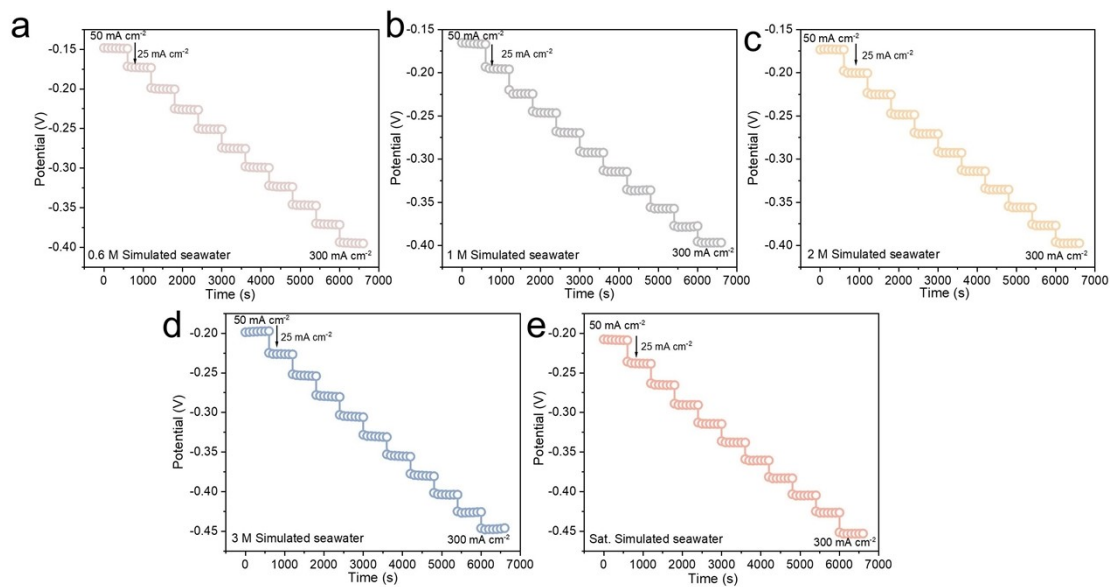


Fig.S24 Multi-step CP tests of  $\text{Co}_8\text{-NiP}_2$  for HER in (a) 0.6 M, (b) 1 M, (c) 2 M, (d) 3 M, (e) saturated simulated seawater.

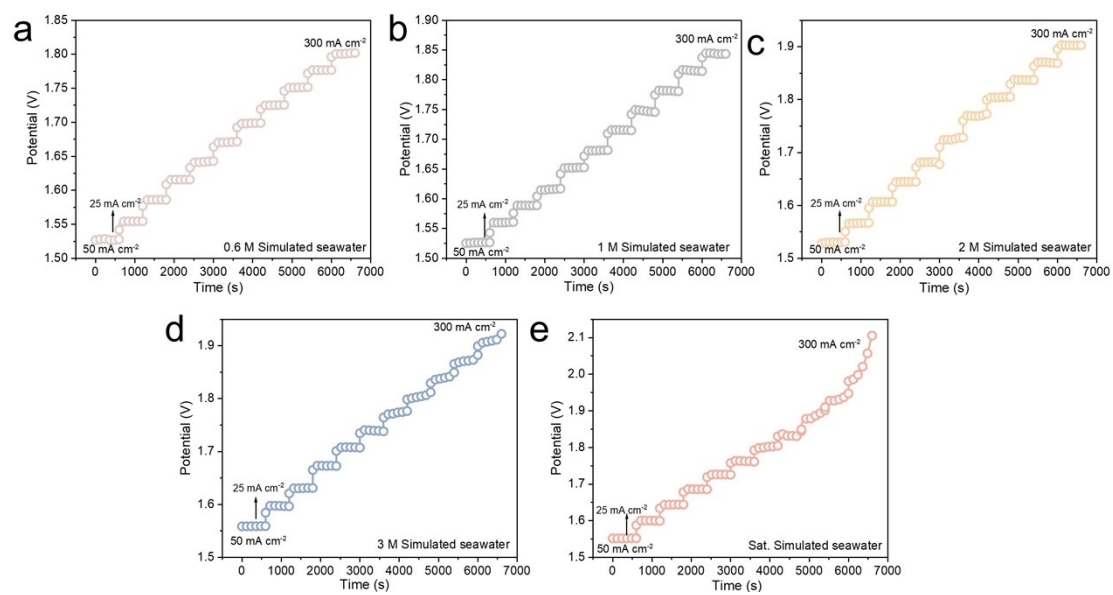


Fig.S25 Multi-step CP tests of  $\text{Co}_8\text{-NiP}_2$  for OER in (a) 0.6 M, (b) 1 M, (c) 2 M, (d) 3 M, (e) saturated simulated seawater.

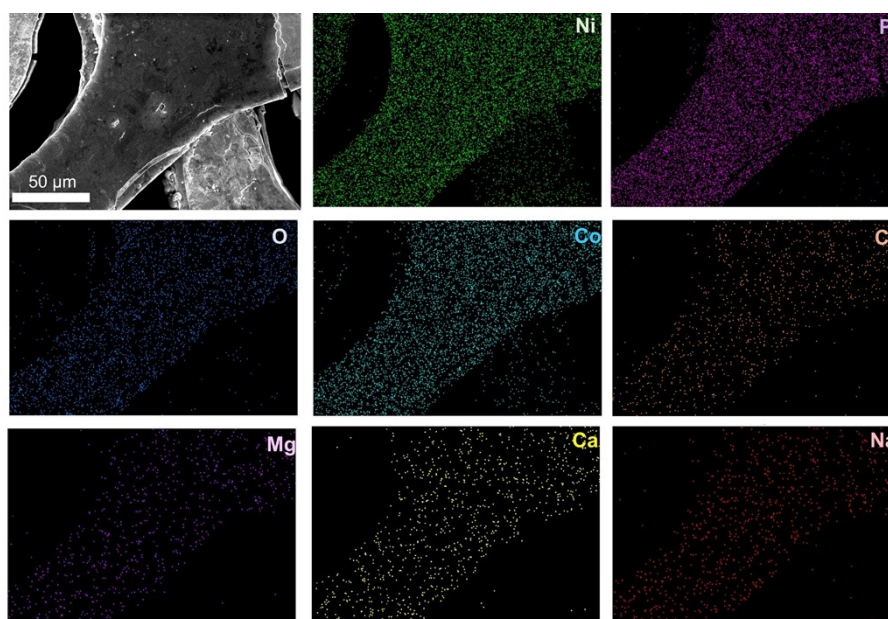


Fig.S26 SEM image and EDS element mapping of  $\text{Co}_8\text{-NiP}_2$  after long-term HER in seawater.

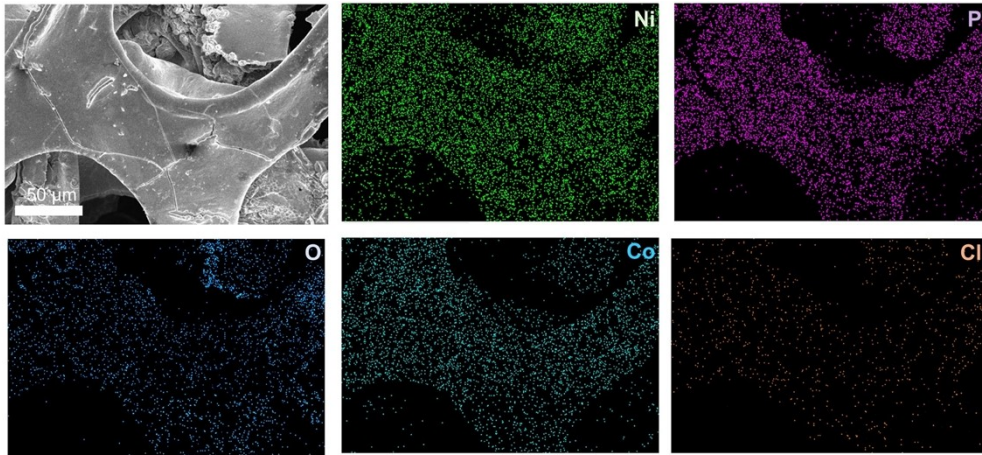


Fig.S27 SEM image and EDS element mapping of  $\text{Co}_8\text{-NiP}_2$  after long-term OER in seawater.

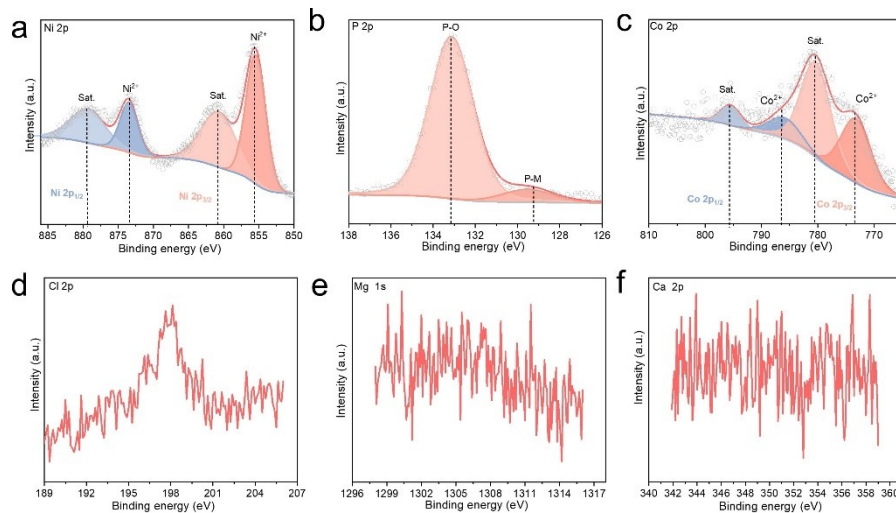


Fig. S28 (a) Ni 2p, (b) P 2p, (c) Co 2p, (c) Cl 2p, (e) Mg 1s and (h) Ca 2p spectrum of

Co<sub>8</sub>-NiP<sub>2</sub> after long-term HER in seawater.

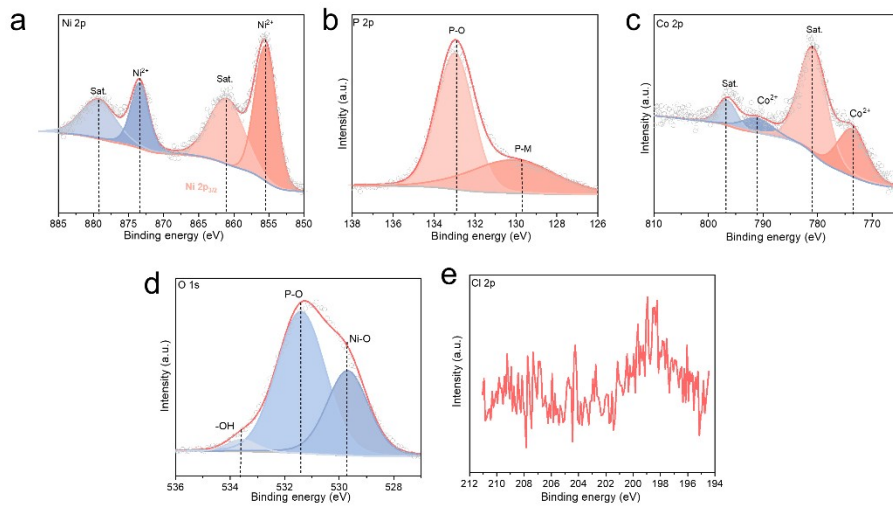


Fig. S29 (a) Ni 2p, (b) P 2p, (c) Co 2p, (d) O 1s and (e) Cl 2p spectrum of  $\text{Co}_8\text{-NiP}_2$  after long-term OER in seawater.

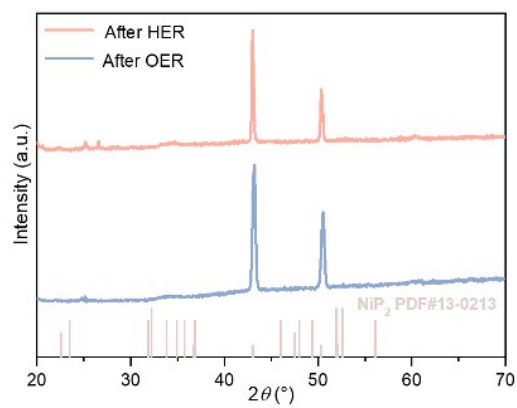


Fig. S30 XRD spectra of  $\text{Co}_8\text{-NiP}_2$  after long-term HER and OER in seawater.

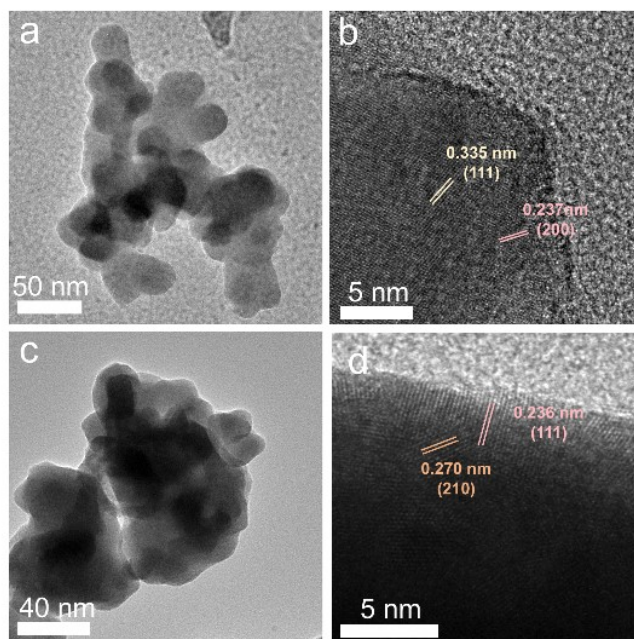


Fig. S31 (a, b) TEM images of  $\text{Co}_8\text{-NiP}_2$  after long-term HER in seawater. (c, d) TEM images of  $\text{Co}_8\text{-NiP}_2$  after long-term OER in seawater.

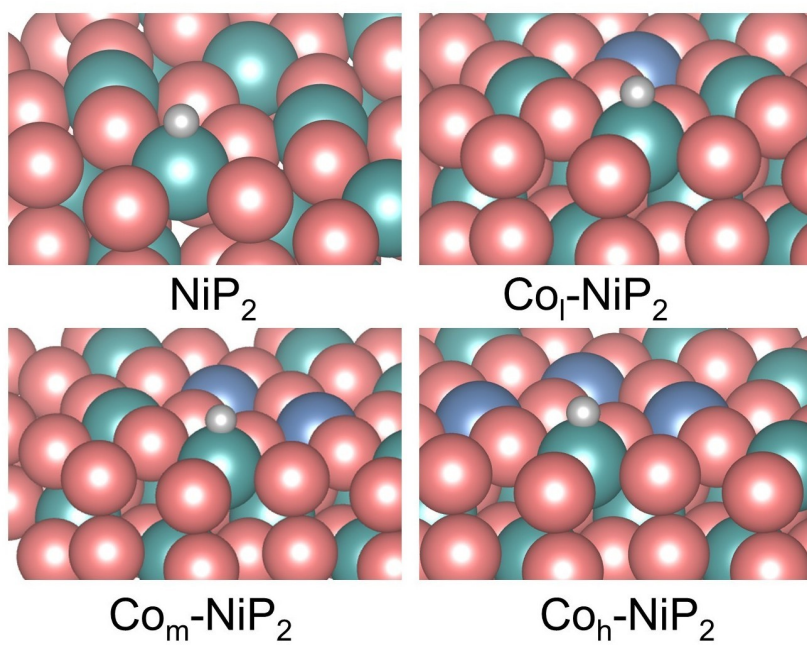


Fig.S32 HER intermediate adsorption model.

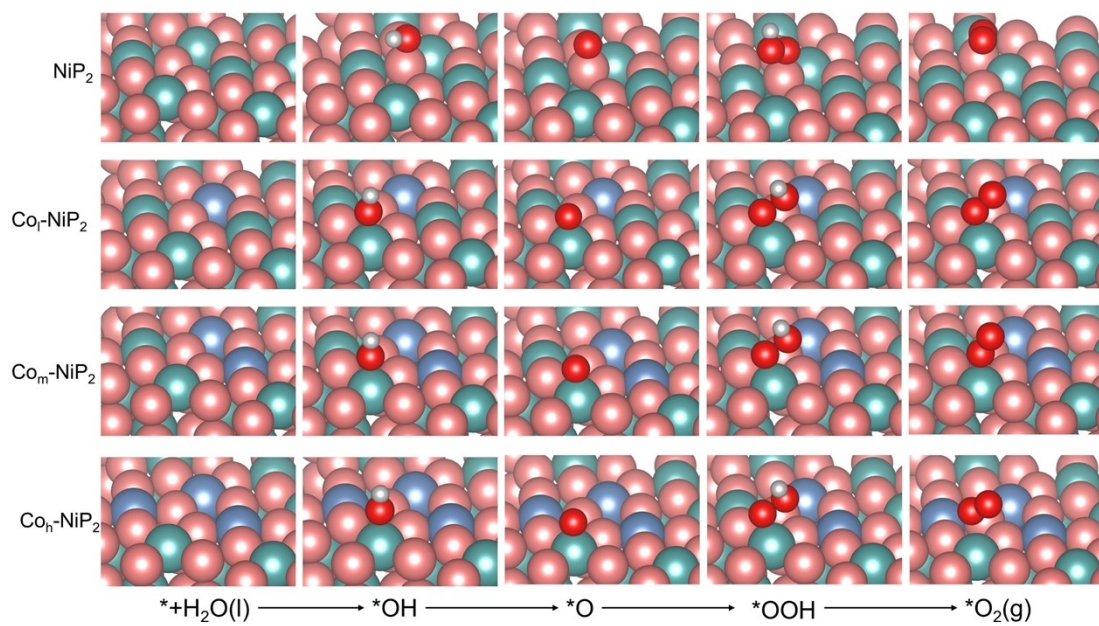


Fig.S33 OER intermediate adsorption model.

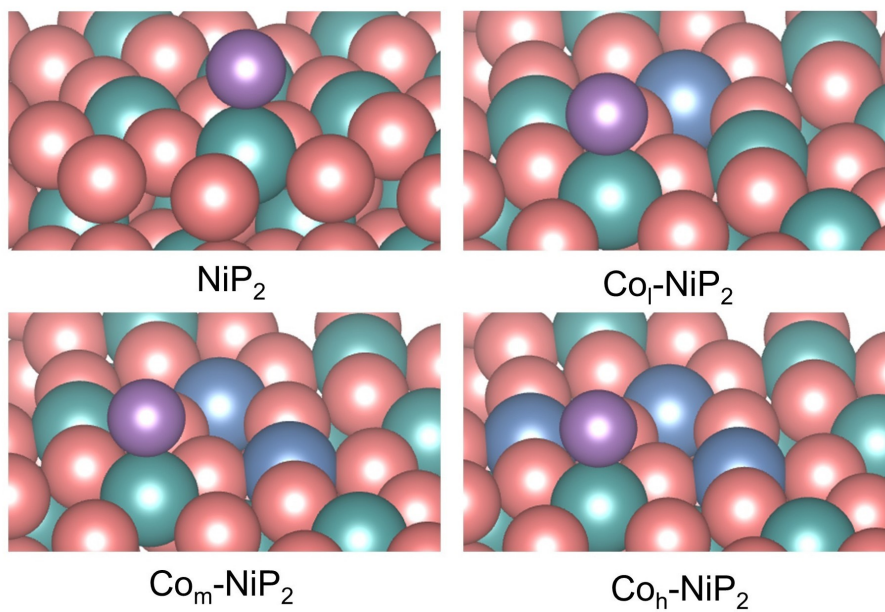


Fig.S34 Cl\* adsorption model.

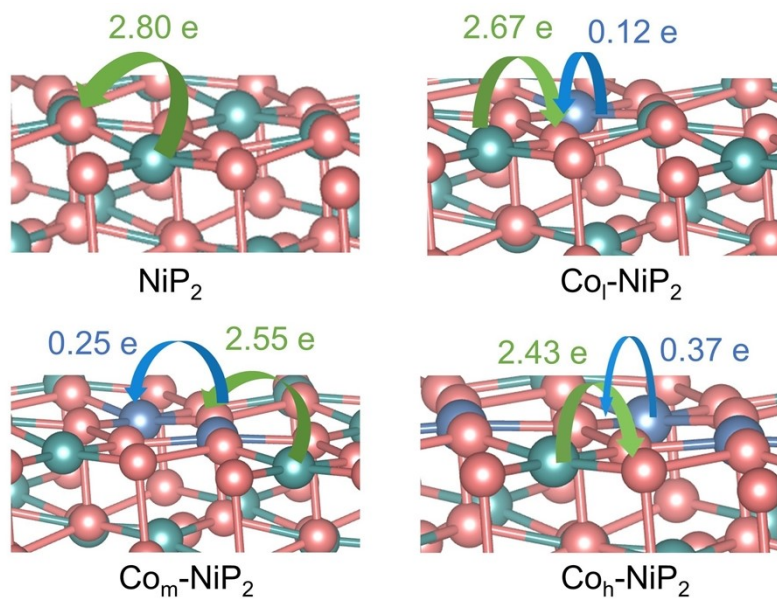


Fig.S35 Average Bader charge transfer quantity of Ni, Co, P (blue: Co→P, green: Ni→P).

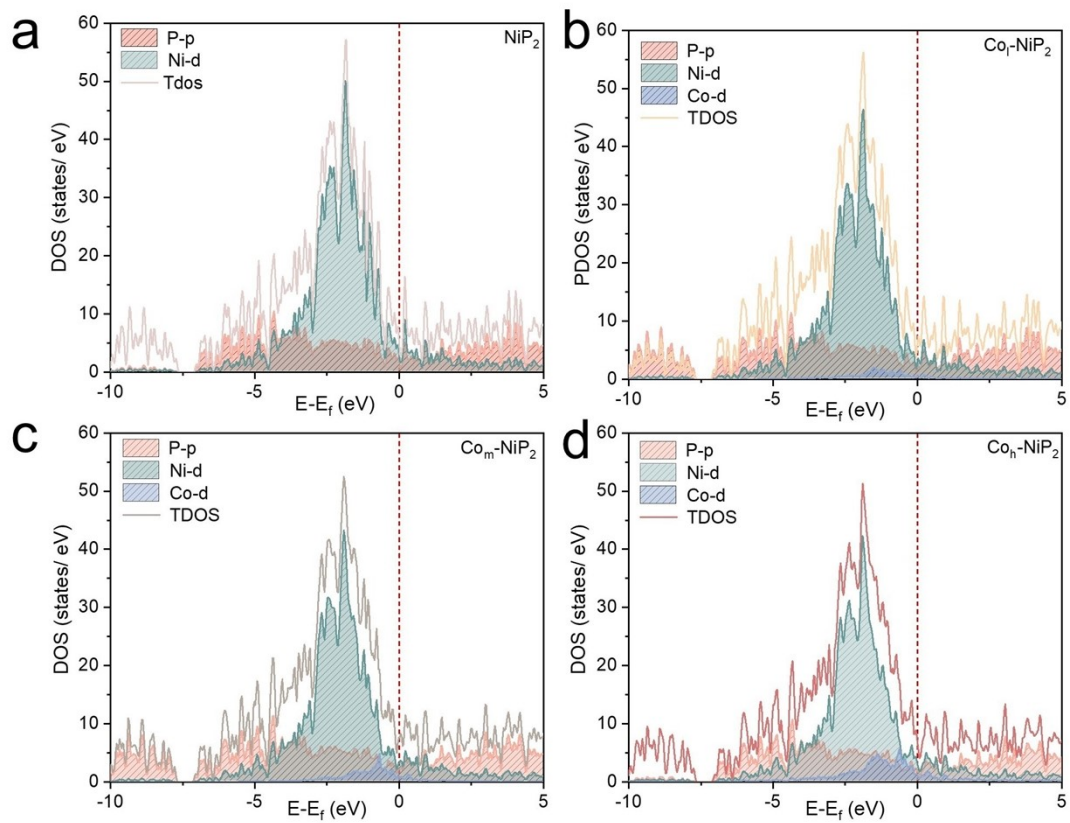


Fig.S36 DOS of (a)  $\text{NiP}_2$ , (b)  $\text{Co}_I\text{-NiP}_2$ , (c)  $\text{Co}_m\text{-NiP}_2$ , (d)  $\text{Co}_h\text{-NiP}_2$

Table S1 The performance of TMP-based HER catalysts reported in recent literature.

Material	electrolyte	electrode	Current density	Overpotential (mV)	Tafel slope (mV dec <sup>-1</sup> )	Reference	
This work	1 M KOH	NF	10	89.7	53.0		
			100	155.2			
			500	252.0			
			1000	352.8			
			100	211			
V-NiP/NiP	1 M KOH	NF	500	293	103	S1	
			1000	334			
CoO-Co <sub>3</sub> O <sub>4</sub> /rGO@NiP	1 M NaOH	Mild steel	10	106.2	107.9	S2	
Ag-AgP/Ni <sub>2</sub> P	1 M KOH	NF	10	78	68.9	S3	
Ni <sub>2</sub> P	1.M KOH	NF	10	159	99.8		
Ni <sub>2</sub> P@C	1.M KOH	NF	10	132	56.29	S4	
Cu-NiP <sub>2</sub>	1.M KOH	NF	10	248	108	S5	
Mn-NiP <sub>2</sub>				233	108		
NPO/NiP	1.M KOH	NF	10	76	213	S6	
				Ti	82		42
				CC	94		49
NiP <sub>x</sub>	1 M KOH	stainless steel	10	97	56	S7	
				97	56		
Por-NiP-Cr	1 M KOH	BDD	50	234	66.72	S8	
			100	252			

Ni <sub>2</sub> P/Ni <sub>5</sub> P <sub>4</sub>	1 M KOH	CC	10	139	62	S9
			100	170		
Ce <sub>0.10</sub> -NiCoP	1 M KOH	NF	10	96	94.75	S10
Ni <sub>2</sub> P/Co <sub>2</sub> P	1 M KOH	NF	10	66	48	S11
Ce-NiP	1 M KOH	NF	10	116	305.9	S12
			100	235		
Fe-Ni <sub>2</sub> P@C	1 M KOH	NF	10	75	45	S13
			1000	313		
Y-NiP	1 M KOH	GP	10	50.6	55	S14
			500	160		
FeCoP/TiN	1 M KOH	CP	500	129	44.9	S15
Co/NiCoP	1 M KOH	-	50	295	92	S16
			300	361		
NiFeP@Ni <sub>2</sub> P/MoO <sub>x</sub>	1 M KOH	-	10	80	131.04	S17
			100	232		
			500	332		
			1000	390		

Table S2 The performance of TMP-based OER catalysts reported in recent literature

Material	electrolyte	electrode	Current density	Overpotential (mV)	Tafel slope (mV dec <sup>-1</sup> )	Reference
			10	207.2		
This work	1 M KOH	NF	100	287.0	67.7	
			300	359		
			500	413		
Ni <sub>2</sub> P@C	1 M KOH	NF	10	279	79	S4
Cu-NiP <sub>2</sub>	1 M KOH	NF	10	276	113	S5
Mn-NiP <sub>2</sub>				271	129	
NPO/NiP	1 M KOH	NF	10	240	116	S6
Ce <sub>0.10</sub> -NiCoP	1 M KOH	NF	10	218	72.12	S10
Ni <sub>2</sub> P-R	1 M KOH	NF	50	379	27.41	S18
MnCr-NiCoP	1 M KOH	NF	10	234.8	50.4	S19
Fe-Ni <sub>2</sub> P	1 M KOH	NF	10	214	36.95	S20
Ce-NiP	1 M KOH	NF	10	276	96	S12
			50	337	93.9	
			10	189		
Ni <sub>7</sub> Fe <sub>3</sub> -Pi	1 M KOH	NF			46.37	S21
			100	286		
Fe-Ni <sub>x</sub> P/RG	1 M KOH	GCE	20	242	44.87	S22
			100	275		
O-M						
Ni <sub>2</sub> P/Fe(	1 M KOH	NF	10	240	57.25	S23

O)OH-40						
(Ni <sub>0.83</sub> Fe <sub>0.17</sub> ) <sub>2</sub> P	1 M KOH	NF	10	215	31.84	S24
P-NiCo-LDH	1 M KOH	NF	10	290	55.05	S25
NiFe:SSP	1 M KOH	FTO	10	248	31	S26
		NF	10	195	31	
Co/NiCoP	1 M KOH	-	300	430	64	S16
P-CoFeLDH	1 M KOH	NF	300	347	48.8	S27
P-CoO <sub>x</sub> /NiFeLDH	1 M KOH	NF	300	265	38.7	S28
Ni <sub>2</sub> P/FeP O <sub>x</sub> /RGO	1 M KOH	GC	100	291		
			500	367	53.8	S29
Fe-Ni <sub>2</sub> P-S/C	1 M KOH	GC	1000	421		
			100	266		
			500	323	52.9	S30
Ce <sub>0.1</sub> -Fe <sub>2</sub> P/NiCoP	1 M KOH	NF	500	280	55.3	S31
NiCo <sub>2</sub> S <sub>4</sub> @Fe <sub>2</sub> P	1 M KOH	-	500	322	44	S32

---

Table S3 The performance of TMP-based catalysts in seawater electrolysis reported in recent literature.

<b>Material</b>	<b>electrolyte</b>	<b>Reaction</b>	<b>Current density</b>	<b>Time (h)</b>	<b>Reference</b>
This work	1 M KOH + seawater	seawater	10	500	
		splitting	300		
V-Ni <sub>2</sub> P/Ni <sub>12</sub> P <sub>5</sub>	Simulated seawater	HER	100	10	S1
Ni <sub>3</sub> S <sub>2</sub> /NiP <sub>x</sub>	1 M KOH + 0.5 M NaCl	seawater	100	200	S33
		splitting			
NiFeP/NiP	Alkaline seawater	seawater	10	500	S34
		splitting			
CoP/Co <sub>2</sub> P	1 M KOH + 0.5 M NaCl	HER	10	25	S35
Ru-Co <sub>2</sub> P	Alkaline seawater	HER	50	30	S36
CNFMPO	1 M KOH + 0.5 M NaCl	seawater splitting	50	15	S37
Ru/C/NiCoP/NF	1 M KOH+0.5 M NaCl	seawater splitting	100	150	S38
Co <sub>2</sub> P-R	1.0 M KOH + seawater	seawater splitting	100	200	S39
Mn-FePV	Alkaline seawater	OER	100	100	S40
Ni <sub>2</sub> P/Co(PO <sub>3</sub> ) <sub>2</sub>	Alkaline seawater	HER	600	60	S41

## Reference

- S1. D. He, L. Cao, J. Huang, X. Zhang, C. Wang, K. Li, K. Kajiyoshi and L. Feng, *Mol. Catal.* 2024, **558**, 114046.
- S2. M. S. Meera, S. Sasidharan, S. George and S. M. A. Shibli, *Appl. Energy Mater.* 2025, **8**, 6001-6015.
- S3. J. Wang, F. Tian, L. Zhang, H. Zhang, J. Fan, L. Zhang, T. Xu and X. Cui, *J. Colloid Interface Sci.* 2024, **673**, 284-290.
- S4. K. Yang, X. Liu, J. Xu, Y. Gong, S. Shen, J. Fan, X. Zhang and Y. Xue, *P Prog. Nat. Sci. Mater. Int.* 2024, **34**, 102-107.
- S5. G. E. Ayom, M. D. Khan, F. M. de Souza, W. Lin, R. K. Gupta and N. Revaprasadu, *J. Energy Storage* 2024, **97**, 112882.
- S6. P. Jiang, B. Zhou, R. He, Y. Li, N. Xu, J. Qiao and D. Ruan, *J. Colloid Interface Sci.* 2024, **669**, 927-934.
- S7. Q. Sun, X. Hao, D. Zhang, T. Zhang, Y. Zhao, X. Huang and X. Liu, *Energy Environ. Mater.* 2024, **7**, e12726.
- S8. R. Zhu, J. Zang, L. Dong, X. Tian, F. Sun, Q. Fu, Z. Zhuang and Y. Wang, *Carbon*, 2025, 120392.
- S9. L. Huang, X. Wei, Y. Yu, D. Sun, Y. Qu, J. Wen, X. Yuan, Q. Su, F. Meng and G. Du, *J. Mater. Sci. Technol.* 2026, 242: 306-316.
- S10. M. Zhang, H. Xu, H. Yang, X. Shang, M. Yuan, Y. Fu, Y. Xiao, S. Wang, X. Wang and B. Jia, *Small*, 2025, 2504837.
- S11. T. Xu, D. Jiao, J. Fan, Y. Dong, Z. Jin, L. Zhang, W. Zhang, J. Zhao, W. Zheng and X. Cui, *Carbon Energy*, 2025, **7**, e668.
- S12. S. Liu, Y. Ye, L. Gao, Z. Yan, H. Pan, Z. Wang, G. Zhang and X. Huang, *Green Chem.* 2025, **27**, 7307-7318.
- S13. D. Li, Z. Li, R. Zou, G. Shi, Y. Huang, W. Yang, W. Yang, C. Liu and X. Peng, *Appl. Catal. B Environ. Energy* 2022, **307**, 121170.
- S14. L. Yang, W. Gou, C. Cheng, Y. Tian, K. Qu, H. Sun, J. Chen, J. Sun and C.-P. Li, *Appl. Surf. Sci.* 2024, **654**, 159505.

- S15. X. Yang, W. Guo, H. Xi, H. Pang, Y. Ma, X. Leng, C. Hou, L. Li, X. Huang and F. Meng, *Adv. Funct. Mater.* 2025, 2505078.
- S16. Y. Lin, X. Cui, Y. Zhao, Z. Liu, G. Zhang and Y. Pan, *Nano Res.* 2023, **16**, 8765-8772.
- S17. Y. Luo, S. Wu, P. Wang, H. Ranganathan and Z. Shi, *J. Colloid Interface Sci.* 2023, **648**, 551-557.
- S18. X. Yu, X. Wang, P. He, G. Yang, F. Qin, Y. Yao, X. Cui and L. Ren, *Energy Environ. Mater.* 2025, e70101.
- S19. Y. Zhang, M. Zhang, H. Zhang, D. Han, J. Wang, R. Yang, C. Zuo and X. Chen, *Fuel*, 2025, **396**, 135348.
- S20. M. Yan, W. Liu, K. Xiang, Y. Li, Y. Zhang, J. Zhang, Y. Ren, Y. Sun, Y. Li and J. Liu, *Inorg. Chem.* 2025, **64**, 9807-9816.
- S21. Y. Zhu, Q. Li, N. Li, M. Lv, F. Xue, M. Dong, K. Lin, J. Deng, J. Zeng and Q. Li, *ACS Sustain. Chem. Eng.* 2025, **13**, 12910-12919.
- S22. Q. Ye, J. Wang, P. Guan, Y. Liu, D. Xu, Y. Zhao and Y. Cheng, *J. Mater. Chem. A*, 2025, **13**, 14293-14303.
- S23. Y. Xing, S. Liu, Y. Liu, X. Xiao, Y. Li, Z. Wang, Y. Hu, B. Xin, H. Wang and C. Wang, *Nano Energy*, 2024, **123**, 109402.
- S24. Z. Wang, S. Liu, J. Du, Y. Xing, Y. Hu, Y. Ma, X. Lu and C. Wang, *Green Chem.* 2024, **26**, 7779-7788.
- S25. J. Zhang, E. Weatherspoon, A. S. Alsubaie, E. Burcar, A. DeMerle, Z. M. El-Bahy and Z. Wang, *Adv. Compos. Hybrid Mater.* 2025, **8**, 72.
- S26. I. Mondal, J. N. Hausmann, S. Mebs, S. Kalra, G. Vijaykumar, K. Laun, I. Zebger, S. Selve, H. Dau and M. Driess, *Adv. Energ. Mater.* 2024, **14**, 2400809.
- S27. G. Huang, Y. Wang, X. Ma, Y. Cao, B. Wei, L. Zhang, W. Chen, F. Ye, C. Xu and X. Du, *J. Taiwan Inst. Chem. Eng.* 2024, **163**, 105664.
- S28. H. M. Xu, C. J. Huang, H. R. Zhu, Z. J. Zhang, T. Y. Shuai, Q. N. Zhan, V. Y. Fominski and G. R. Li, *Small*, 2024, **20**, 2400201.
- S29. Y. Liu, L. Ji, D. Xu, Q. Ye, Y. Zhao and Y. Cheng, *J. Colloid Interface Sci.* 2025, **683**, 474-483.
- S30. Z. Wang, K. Wang, Y. Pan, Q. Ye, C. Zhang, D. Zhang, Y. Zhao and Y. Cheng, *J. Colloid*

- Interface Sci. 2025, **678**, 886-896.
- S31. F. Zhang, K. Wang, H. Zhang, S. Yang, M. Xu, Y. He, L. Lei, P. Xie and X. Zhang, Adv. Funct. Mater. 2025, 2500861.
- S32. A. B. Ali, T. A. Ahmed, F. Alimova, R. Jhala, P. R. Rao, J. Nanda, A. Painuly, A. Singh, A. S. Shaik and S. Islam, Synth. Met. 2025, 117962.
- S33. J. Zhang, M. Sun, Y. Jiang, Y. Su, T. Zhao, Q. Lu and G. Yin, Chin. J. Chem. 2025, **43**, 3109-3118.
- S34. S.-Y. Lu, L. Wang, C. Wu, J. Zhang, W. Dou, T. Hu, R. Wang, Y. Liu, Q. Yang and M. Jin, Inorg. Chem. Front. 2024, **11**, 3187-3199.
- S35. J.-B. Chen, H. Wang, Y.-X. Xiao and J. Ying, Chem. Mater. 2025, **37**, 2145-2154.
- S36. B. Jiang, H. Xiao, J. Li, H. Tang, H. Chen, S. Deng, Y. Tan, C. Yu, J. Wang and A. Huang, Small, 2025, **21**, 2406900.
- S37. H.-M. Zhang, L. Zuo, Y. Gao, J. Guo, C. Zhu, J. Xu and J. Sun, J. Mater. Sci. Technol. 2024, **173**, 1-10.
- S38. Z. Liu, X. Ning, A. Hao, M. F. Khan and S. Rehman, ChemSusChem, 2025, **18**, e202401197.
- S39. X. Wang, T. Su, Z. Lu, L. Yu, N. Sha, C. Lv, Y. Xie and K. Ye, J. J. Colloid Interface Sci. 2025, **691**, 137389.
- S40. K. Wang, X. Liu, Q. Yu, X. Wang, J. Zhu, Y. Li, J. Chi, H. Lin and L. Wang, Small, 2024, **20**, 2308613.
- S41. M. Zhang, W.-Z. Chen, Z. Liu, J. He and Y.-Q. Wang, Int. J. Hydrog. Energy. 2023, **48**, 17783-17800.